C. R. Physique 14 (2013) 629–635

Contents lists available at SciVerse ScienceDirect

Comptes Rendus Physique

www.sciencedirect.com

Trends and perspectives in solid-state wetting / Mouillage solide–solide : tendances et perspectives

Droplet spreading: Theory and experiments

Étalement de gouttelettes : théorie et expériences

Michael J. Davis *, Stephen H. Davis

Department of Engineering Sciences and Applied Mathematics, McCormick School of Engineering Science and Applied Science, Northwestern University, Evanston, IL 60208, USA

ARTICLE INFO

Article history:
Available online 6 August 2013

Keywords:
Spreading
Wetting
Contact lines

Mots-clés :
Dispersion
Mouillage
Lignes de contact

ABSTRACT

A hypothesis is presented that distinguishes the characteristics of spreading by hydrodynamic forces from those driven by molecular/kinetic effects, demarking the regimes by contact-line speeds and contact angles. Several applications of the criterion to experiments are discussed.

RÉSUMÉ

Une hypothèse est présentée, qui différencie l'étalement produit par des forces hydrodynamiques de celui engendré par des effets cinétiques ou moléculaires, permettant ainsi de séparer les régimes suivant les vitesses des lignes de contact et les angles de raccordement. Ce critère est discuté dans le cas de plusieurs applications expérimentales.

1. Introduction

The spreading of a clean, isothermal, liquid drop on a smooth, planar substrate stands as a prototype system for studying the dynamics of moving contact lines. It involves the surface energies of all the interfaces and hence the wettability properties of the materials.

The spreading of liquids on solids has much scientific interest in that the regions near the contact lines, the three-phase lines, are the sites of the interaction of microscopic chemistry and physics with the large scale, continuum behavior of the droplets. The spreading of liquids on solids has much engineering interest ranging from coatings, soldering, and printing to micro/nanotechnology, optics, and brazing.

The hydrodynamic theory (HDT) describing such dynamics dates to the 1970's [1,2]. Huh and Scriven [1] studied a wedge flow and identified the existence of a non-integrable singularity in the rate-of-strain tensor. They listed a number of potential causes of the singularity including the no-slip condition at the solid–liquid interface. Dussan V and Davis [2] examined the kinematics of moving contact lines *in general* and showed that contact-line motion is impossible if the no-slip condition holds, and further showed that the drop rolls along the solid. Since this time, there have been many investigations that generalize these models with new effects in the continuum theory [3,4] (temperature and composition gradients including Marangoni effects and evaporation). Further, molecular dynamics [5,6] has been used to explore smaller

* Corresponding author.
E-mail address: davis@u.northwestern.edu (M.J. Davis).

1631-0705/$ – see front matter
http://dx.doi.org/10.1016/j.crhy.2013.06.011

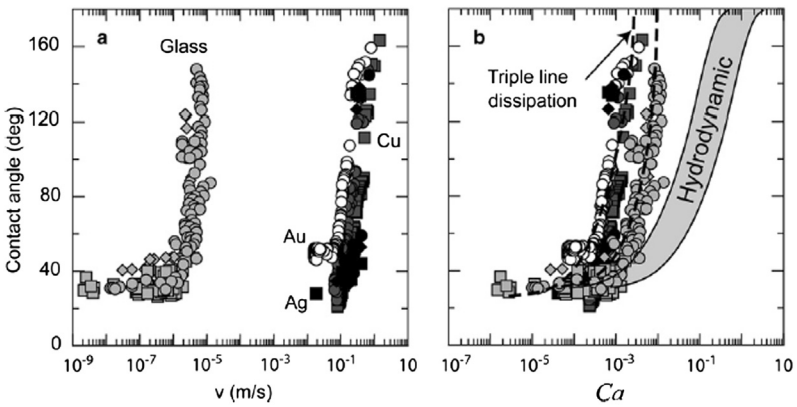

Fig. 1. Contact angle versus (a) contact-line speed, and (b) capillary number. In (b), the gray area corresponds to the HDT, while the dashed lines correspond to the MKT with the distance λ between adsorption sites comparable to interatomic distances (1–3 Å) and wetting activation energies $\Delta G_w \approx 100$ kJ/mol for metals and $\Delta G_w \approx 230$–300 kJ/mol for glasses.

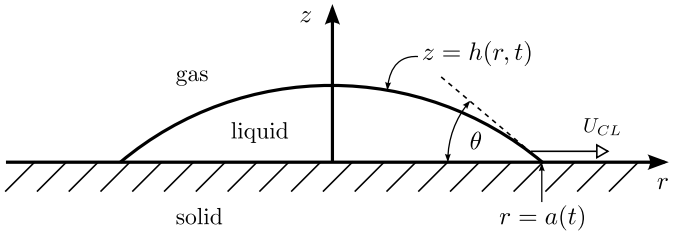

Fig. 2. A liquid droplet spreading on a smooth, planar substrate.

scales than describable by continuum theory. The predictions of all these theories have been shown to agree quantitatively with the spreading of organic liquids on glass [7–9].

There is a second approach to spreading which involves zero bulk flow of the liquid but instead postulates that molecules from the liquid near the contact-line jump across and attach to the substrate effectively moving the contact line forward; this gives the molecular kinetic theory (MKT) [10,11].

Saiz and Tomsia [12,13] performed a series of experiments on molten glasses and liquid metals spreading on molybdenum substrates. Their results [13] shown in Fig. 1 show the spreading dynamics, contact angle as a function of contact-line speed in (a) and the same data, contact angle as a function of capillary number in (b). In (b), the gray area indicates the HDT curves for a range of slip coefficients clearly showing that the theory is inapplicable here. The dashed curves represent the MKT result for appropriate parameter values (see caption), showing that the MKT works well. This work, plus others that followed, establish that the MKT as well as the HDT apply to categories of systems and which one does apply can be determined after the experiments have been analyzed.

The present paper describes no new theory nor experiment, but instead organizes the known theories in a way to clarify the issues. The outcome is a criterion that defines which theory applies *before* the experiments are performed, given the properties of the three materials (liquid, vapor, solid) involved. It also shows that *both* theories can apply to a *given* experiment at different times, at different contact angles, and at different contact-line speeds, although in certain experiments one of the theoretical ranges may be so small as to be unobservable.

2. Two theories

The theories described earlier are well known in the community so they merely need to be sketched here to emphasize certain points.

2.1. Hydrodynamic theory (HDT)

Fig. 2 shows a liquid droplet on a smooth substrate. The geometry can be axi-symmetric or two-dimensional; only the former will be outlined here.

The bulk liquid dynamics are described by Stokes flow (Navier–Stokes with inertia absent) and conservation of mass for liquids of constant density

$$\mu\nabla^2\mathbf{v} - \nabla p = 0, \quad \nabla\cdot\mathbf{v} = 0 \tag{1}$$

where μ is the dynamic viscosity of the liquid, $\mathbf{v} = (u, w)$ is the velocity vector in direction (r, z), and p is the pressure. The surrounding vapor is considered passive. The effect of gravity is neglected, appropriate for droplets smaller than a couple of millimeters.

On the liquid–vapor interface, $S : z = h(r, t)$, is the kinematic boundary condition

$$\mathbf{v} \cdot \mathbf{n} = \frac{\partial h}{\partial t} \tag{2a}$$

where $\mathbf{n}$ is the unit normal vector to S pointing out of the liquid, and the stress conditions are as follows:

$$\mu \mathbf{D} \cdot \mathbf{n} \cdot \mathbf{t}^j = 0 \tag{2b}$$

$$P_{\mathrm{A}} - P + \mu \mathbf{D} \cdot \mathbf{n} \cdot \mathbf{n} = \gamma \kappa \tag{2c}$$

where P_{A} is the pressure in the vapor, $\mathbf{t}^j$ $(j = 1, 2)$ are the unit tangent vectors to S, $\mathbf{D}$ is the rate of deformation tensor of the liquid, γ is the surface tension on S, and κ is the mean curvature of S.

On the contact line (CL) at $r = a(t)$, S has zero height:

$$h(r, t) = 0 \quad \text{on } r = a(t) \tag{3a}$$

and the contact angle θ is related to the slope of S at $r = a(t)$,

$$\frac{\partial h}{\partial r} = -\tan\theta \quad \text{at } r = a(t) \tag{3b}$$

On the wetted area, $z = 0$, $r \leqslant a(t)$, there is no penetration of liquid and a slip condition

$$w = 0 \tag{4a}$$

$$u = \beta \frac{\partial u}{\partial z} \tag{4b}$$

where β is the (numerically small) slip coefficient. Note that other slip laws have been used in the literature and it has been found by [14] that the precise form used has negligible effect on the macroscopic (continuum) behavior of the spreading. Of course one cannot set $\beta = 0$ for then $\mathbf{D}$ has a non-integrable singularity [1,2].

Finally, there is volume conservation

$$V_0 = 2\pi \int_0^{a(t)} r h(r, t)\, \mathrm{d}r \tag{5}$$

There are two small parameters in the problem, the capillary number Ca given by:

$$Ca = \frac{\mu U_{\mathrm{CL}}}{\gamma} \tag{6a}$$

where U_{CL} is a measure of the speed of the CL, and a nondimensional slip coefficient $\hat{\beta}$.

The solution of the system (1)–(5) requires singular perturbation analysis [15–17], and according to [15], for $Ca \to 0$ and $\hat{\beta} \to 0$,

$$g(\theta) - g(\theta_{\mathrm{A}}) = Ca \log \frac{L}{\beta} \tag{6b}$$

where g is a known function, L measures the droplet size, θ is the macroscopic contact angle and θ_{A} is the advancing contact angle. A more useful version of (6b) holds for $\theta < 3\pi/4$,

$$K_{\mathrm{HD}}\left(\theta^3 - \theta_{\mathrm{A}}^3\right) = U_{\mathrm{CL}} \tag{7a}$$

where

$$K_{\mathrm{HD}} = \frac{9\mu}{\gamma} \log \frac{L}{\beta} \tag{7b}$$

From these results one can calculate appropriate power-law or exponential spreading rates.

2.2. Molecular kinetic theory (MKT)

According to [10,11], the contact line can advance absent bulk liquid flow. Based on attachment–detachment of molecules, there can be forward motion that satisfies

$$U_{\mathrm{CL}} = 2\xi^0\lambda \sinh\left[\frac{\gamma\lambda^2}{2kT}\gamma(\cos\theta_{\mathrm{A}} - \cos\theta)\right] \tag{8a}$$

where λ is the molecular displacement, ξ^0 is its frequency, and T is the absolute temperature. Here:

$$\xi^0 = \frac{k}{h}\exp\left(\frac{\Delta G_{\mathrm{w}}}{NkT}\right) \tag{8b}$$

ΔG_{w} is the wetting energy, and k is the Boltzmann constant. Again, one can find a simpler form, this time if $|\theta - \theta_{\mathrm{A}}|$ is small, viz.,

$$U_{\mathrm{CL}} = K_{\mathrm{MK}}\left(\theta^2 - \theta_{\mathrm{A}}^2\right) \tag{9a}$$

where

$$K_{\mathrm{MK}} = \frac{\xi^0\lambda^3\gamma}{2kT} \tag{9b}$$

By comparing the results of numerical simulation and experiments of spreading at high temperatures, [18,19] have concluded that the MKT applies but that the physical phenomenon involves the jumping between ordered layers of atoms at the solid/liquid interface. In either this or the previous case, Eqs. (8)–(9) should still apply.

2.3. The crossing point

Consider now a spreading experiment in which all the parameters in K_{HD} and K_{MK} are known a priori. One can ask, where do curves (7) and (9) cross?

One solution is the long-time state $\theta^* = \theta_{\mathrm{A}}$ in which the drop has reached equilibrium. The other solutions $\theta^* \neq \theta_{\mathrm{A}}$ satisfy:

$$K_{\mathrm{HD}}\left(\theta^{*2} + \theta^*\theta_{\mathrm{A}} + \theta_{\mathrm{A}}^2\right) = K_{\mathrm{MK}}\left(\theta^* + \theta_{\mathrm{A}}\right) \tag{10}$$

which can be rescaled to the quadratic equation:

$$\left(\frac{\theta^*}{\tilde{K}}\right)^2 - (1-\tilde{\theta}_{\mathrm{A}})\frac{\theta^*}{\tilde{K}} - \tilde{\theta}_{\mathrm{A}}(1-\tilde{\theta}_{\mathrm{A}}) = 0 \tag{11a}$$

where

$$\tilde{\theta}_{\mathrm{A}} = \frac{\theta_{\mathrm{A}}}{\tilde{K}} \tag{11b}$$

$$\tilde{K} = \frac{K_{\mathrm{MK}}}{K_{\mathrm{HD}}} \tag{11c}$$

Eq. (11a) is easily solved for $\theta^*/\tilde{K}$ as a function of $\tilde{\theta}_{\mathrm{A}}$ giving the curve shown in Fig. 3(a). If this solution is substituted into, say, Eq. (9a), one can find U_{CL} as a function of $\tilde{\theta}_{\mathrm{A}}$, as shown in Fig. 3(b). Note that here θ_{A} is measured in radians. One can notice that in Fig. 3(b), U_{CL} can be negative for $\tilde{\theta}_{\mathrm{A}} < 2/3$; this is the case corresponding to a receding contact line. Fig. 4 shows the plots and their intersections. At this point we state explicitly our hypothesis.

Hypothesis: The two theories, HDT and MKT, both predict θ versus U_{CL}. Clearly, at high values of U_{CL}, the HDT should apply, and at low values, the MKT should apply. The claim here is that each of these persists until the intersections $(U_{\mathrm{CL}}^*, \theta^*)$, and the applicable theory can be determined a priori from the plotted characteristics in Fig. 4.

In Fig. 4, the arrows indicate the presumed parameter trajectories of a given spreading evolution. As time increases, U_{CL} decreases and θ does as well, and as $t \to \infty$, $\tilde{\theta} \to \tilde{\theta}_{\mathrm{A}}$. There are several possibilities generated by Fig. 4. If there is complete spreading as shown in Fig. 4(a), as one moves from right to left in the experiment and the path HDT for "large" speed is followed because the bulk shear will be significant, whereas it follows the path MKT for "small" speed, $U_{\mathrm{CL}} < U_{\mathrm{CL}}^*$. There are also partial-wetting cases, Fig. 4(b) for $0 < \tilde{\theta}_{\mathrm{A}} < 2/3$ that show a similar scenario for θ_{A} not too large and usually $U_{\mathrm{CL}} \geqslant 0$. Notice that near the origin the crossing at $\theta^* = \theta_{\mathrm{A}}$ gives rise to a small region of $U_{\mathrm{CL}} < 0$. Fig. 4(c) shows the case $2/3 < \tilde{\theta}_{\mathrm{A}} < 1$, which from Fig. 3(b) shows that θ^* occurs when $U_{\mathrm{CL}} < 0$. If the experiment begins at positive U_{CL}, the HDT path is followed to θ_{A} and $U_{\mathrm{CL}} = 0$, but if it begins at negative U_{CL}, an unlikely event, the trajectory begins on path MKT,

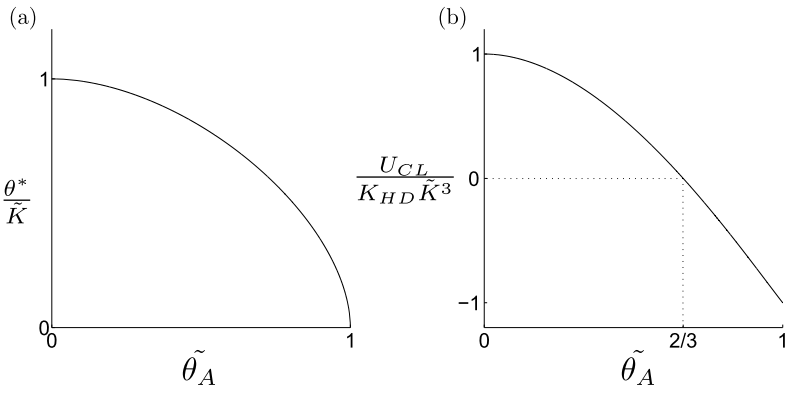

Fig. 3. Critical spreading conditions at crossing; showing (a) contact angle, and (b) contact-line speed, assuming no contact-angle hysteresis.

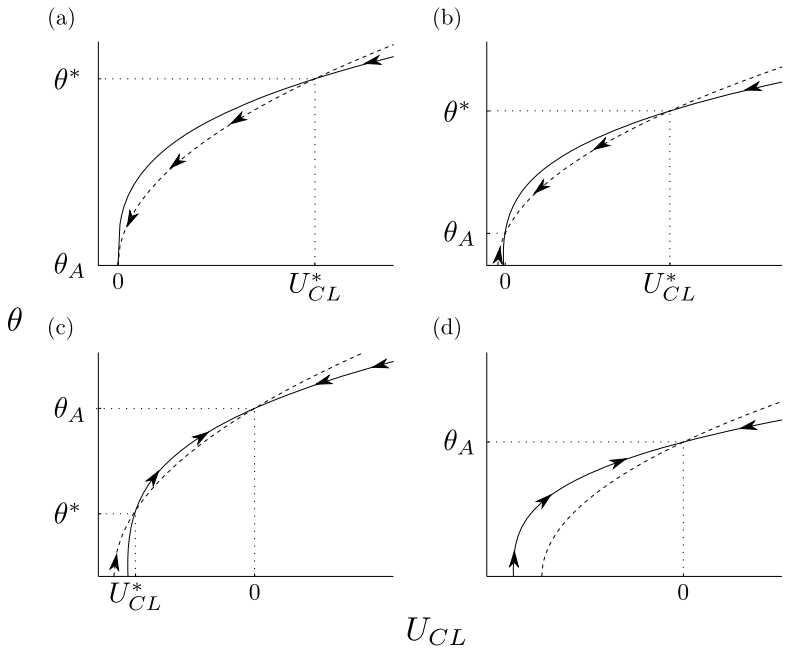

Fig. 4. Characteristic spreading according to Eqs. (7) (HDT, solid) and (9) (MKT, dashed) for (a) $\tilde{\theta}_A = 0$, (b) $0 < \tilde{\theta}_A < 2/3$, (c) $2/3 < \tilde{\theta}_A < 1$, and (d) $\tilde{\theta}_A > 1$, assuming no contact-angle hysteresis.

switches to HDT at θ^*, and approaches θ_A from negative values of U_{CL}. Finally, Fig. 4(d) shows the case of large θ_A in which $\tilde{\theta}_A > 1$. Here, there is a crossing at $\theta^* = \theta_A$, $U_{CL} = 0$, but no other, and the trajectory is attracted there.

Thus, as one moves from right to left, the experiment will follow the HDT curve for "large" speed because that theory depends on bulk shear flow whereas it may follow the MKT curve for "small" speed. The next section tests this hypothesis by comparing to experiments. If the hypothesis outlined is correct, then in principle, spreading in most experiments passes from an HDT regime to an MKT regime, though in limiting cases one of these may disappear or be so small as to be unobservable.

In Section 3, experimental observations are related to Fig. 4 which are obtained using the simplified Eqs. (7a) and (9a), chosen for clarity, and should be quite good for comparisons. Clearly, the more exact versions, Eqs. (6a) and (8a) could be used instead for more accuracy.

3. Comparison with experiment

The key numerical value that emerges is the ratio of K-values, $\tilde{K} = K_{MK}/K_{HD}$. If $\tilde{K}$ is large, most of the lifetime of the spreading resides in the MKT domain and conversely, if it is small, the HDT domain contains the major part of the lifetime, depending on the size of θ_A. (As shall be seen, large means unity or more.) The implication here is that if $0 < \tilde{K} < \infty$, both domains should be present but not necessarily observable.

Example 1. Consider the case of droplets of silicone oil spreading on a clean, glass substrate. Here, there is complete wetting, so that $\theta_A = 0$. This is the system that laid the basis for the HDT because it showed quantitative agreement between theory and experiment, giving Tanner's law [7] for the contact-line speed,

$$U_{CL} = k'_A \theta^3 \tag{12}$$

where k'_A is a constant. This has been generalized to the cases in which materials are chosen with $\theta_A \neq 0$, and

$$U_{CL} = k''_A \left(\theta^3 - \theta_A^3\right) \tag{13}$$

where k''_A is another constant, verified both in theory [20–22] and experiment [3,8,9].

In the first case (see Fig. 4(a)), $\theta_A = 0$ and $\theta^* = \tilde{K}$ which is essentially zero, so that as seen, the HDT holds nearly everywhere. Here, $10^{-4} < \tilde{K} < 10^{-3}$ with capillary number $2 \times 10^{-7} < Ca < 2 \times 10^{-1}$, consistent with the small-Ca HDT.

Example 2. A large series of experiments have examined the spreading of drops of liquid metals and molten salts, all on substrates of Mo [12,13,23]. A subset of these lead to Fig. 1(a) for measured contact angle as a function of U_{CL}. Fig. 1(b) shows the same data compared to the MKT predictions. The shaded region gives the predicted region using the HDT, clearly showing its inapplicability here.

As a sample case consider the spreading of liquid gold (Au) at $T = 1100\,^\circ$C on Mo. Here $\theta_A = 24^\circ$ and $\tilde{K} = 34$ so that $\tilde{\theta}_A = 0.42$ and the MKT describes (see Fig. 4(b)) the spreading everywhere except possibly at very small time in which the HDT might hold. The surmise that the spreading satisfies MKT is consistent not only for this case of an Au droplet but for the entire set of experiments cited.

Example 3. Another sample case consists of molten glass at $T = 1250\,^\circ$C on Mo. Here, $\theta_A = 39^\circ$ and now $\tilde{K} = 1.8$ so that $\tilde{\theta}_A = 0.68$, Fig. 4(c) applies, and so the MKT is a correct descriptive of the experimental data.

Example 4. Consider the spreading of a liquid drop of silver (Ag) at $T = 1070\,^\circ$C on Mo with $\theta_A = 26^\circ$. Here, $\tilde{K} = 1.1$, and hence, the MKT theory will define the spreading for a significant portion of the experiment (see Fig. 4(b)). The latter behavior is consistent with the observations in [12,13]. This case might be a good one for observing experimentally the change from HDT to MKT behavior.

Example 5. Consider dibutyl phthalate at room temperature spreading on a substrate of PET [24]. Here, $\theta_A \leqslant 5^\circ$, $\theta^* = \tilde{K}$, and $Ca = 7 \times 10^{-9}$ so that by present hypothesis the HDT should apply everywhere, given that $\tilde{K} = 2 \times 10^{-4}$. Here, $\tilde{\theta}_A \leqslant 436$ so Fig. 4(d) applies.

This conclusion is opposite that of [24] who conclude that at early times (higher speed) that MKT holds and later (low speeds) the HDT holds. Their conclusions seem to violate ones' intuition regarding the ranges of applicability of the theories.

4. Conclusions

This paper presents a hypothesis that should enable one to anticipate *before* an experiment is performed the quantitative behavior of a spreading drop regardless of the materials chosen. In the most general case the droplet spreading occupies two different regimes. At "early" times the contact-line speed is "large", the contact angle is "large", and the droplet rolls along the substrate so that the HDT applies. As time goes on, the contact-line speed U_{CL} decreases as does the contact angle θ. When the operating point of Fig. 4(a) and (b) crosses the point θ^*, the motion changes from that of HDT to MKT. Now, U_{CL} is "small", θ is small, and the dominant mechanism for contact-line motion involves molecular hopping rather than hydrodynamics.

These two dynamic regimes are generally present in spreading experiments though one of these may be absent or so small as to be non-observable.

This hypothesis involves the calculation of one number, $\tilde{K} = K_{MK}/K_{HD}$, which involves the material parameters of the liquid, the solid, and the vapor, and may be used to design experiments that display certain phenomena of interest. For example one could select materials explicitly displaying the transition from HDT to MKT. Further, given parametric variations of $\tilde{K}$, one might be able to alter the droplet environment in order to emphasize one regime over the other, and even add physical effects that create a cessation of spreading even when $\theta_A = 0$. An example of this is when thermal variations of surface tension cause thermocapillary stresses [3,22] that oppose the spreading by HDT.

In Figs. 3 and 4 there are regions of parameter space in which $U_{CL} < 0$ and so the contact line is receding. In such cases Eqs. (7a) and (9a) should have θ_A replaced by θ_R, the receding contact angle. Now because in this region $\theta < \theta_R$, $U_{CL} < 0$, as it should be.

When contact-angle hysteresis is absent, $\theta_A = \theta_R$, and so the outlined theories and figures are as described above. When contact-angle hysteresis is present, so that $\theta_A > \theta_R$, there will be local changes in Fig. 4 near points where $U_{CL} = 0$. For example, in Fig. 4(c), as the trajectory approaches $U_{CL} = 0$ from the left, it approaches θ_R whereas from the right it approaches θ_A.

The solid curve would then have a jump discontinuity at $U_{CL} = 0$. However, the described hypothesis regarding changes in mechanism of spreading at crossing points still holds.

There have been a number of experiments, e.g. [25,26], at high temperature in which the substrate is not planar and passive but instead exhibits chemical reaction between the droplet and the substrate. Apart from early-spreading times, during which little reaction has occurred, such spreading would likely follow a parametric path different from HDT or MKT. This would then open the possibility of yet another transition in addition to HDT to MKT.

Acknowledgement

S.H.D. is pleased to acknowledge the helpful comments of Eduardo Saiz on an earlier version of the manuscript.

References

[1] C. Huh, L.E. Scriven, Hydrodynamic model of steady movement of a solid/liquid/fluid contact line, J. Colloid Interface Sci. 35 (1971) 85–101.
[2] E.B. Dussan V, S.H. Davis, On the motion of a fluid–fluid interface along a solid surface, J. Fluid Mech. 65 (1974) 71–95.
[3] P. Ehrhard, Experiments on isothermal and non-isothermal spreading, J. Fluid Mech. 257 (1993) 463–483.
[4] D.M. Anderson, S.H. Davis, The spreading of volatile liquid droplets on heated surfaces, Phys. Fluids 7 (1995) 248.
[5] M.O. Robbins, P.A. Thompson, Molecular dynamics simulations of contact line motion, Mater. Res. Soc. Symp. Proc. 177 (1990) 411–422.
[6] J. Yang, J. Koplik, J.R. Banavar, Molecular dynamics of drop spreading on a solid surface, Phys. Rev. Lett. 67 (1991) 3539–3542.
[7] L.H. Tanner, The spreading of silicone oil drops on horizontal surfaces, J. Phys. D: Appl. Phys. 12 (1979) 1473–1484.
[8] A.M. Cazabat, M.A. Cohen Stuart, Dynamics of wetting: Effects of surface roughness, J. Phys. Chem. 90 (1986) 5845–5849.
[9] J.D. Chen, Experiments on a spreading drop and its contact angle on a solid, J. Colloid Interface Sci. 122 (1988) 60–72.
[10] T.D. Blake, J.M. Haynes, Kinetics of liquid/liquid displacement, J. Colloid Interface Sci. 30 (1969) 421–423.
[11] T.D. Blake, J.C. Berg, Kinetics of Liquid/Liquid Displacement, Marcel Dekker, New York, 1993, pp. 251–309.
[12] E. Saiz, A.P. Tomsia, Atomic dynamics and Marangoni films during liquid-metal spreading, Nat. Mater. 3 (2004) 903–909.
[13] E. Saiz, A.P. Tomsia, Kinetics of high-temperature spreading, Curr. Opin. Solid State Mater. Sci. 9 (2005) 167–173.
[14] E.B. Dussan V, The moving contact line: The slip boundary condition, J. Fluid Mech. 77 (1976) 665–684.
[15] R.G. Cox, The dynamics of the spreading of liquids on a solid surface. Part 1. Viscous flow, J. Fluid Mech. 121 (1982) 169–194.
[16] O.V. Voinov, Hydrodynamics of wetting, Izv. Akad. Nauk SSSR, Meh. Židk. Gaza 5 (1976) 76–84.
[17] L.M. Hocking, A.D. Rivers, Spreading of a drop by capillary action, J. Fluid Mech. 168 (1986) 425–442.
[18] M. Benhassine, E. Saiz, A.P. Tomsia, J. De Coninck, Nonreactive spreading at high-temperature revisited for metal systems via molecular dynamics, Langmuir 25 (2009) 11450–11458.
[19] M. Benhassine, E. Saiz, A.P. Tomsia, J. De Coninck, Role of substrate commensurability on non-reactive wetting kinetics of liquid metals, Acta Mater. 58 (2010) 2068–2078.
[20] J. Lopez, C.A. Miller, E. Ruckenstein, Spreading kinetics of liquid drops on solids, J. Colloid Interface Sci. 56 (1976) 460–468.
[21] V.M. Starov, Spreading of droplets of nonvolatile liquids over a flat solid surface, Colloid J. USSR 45 (1983) 1009–1015.
[22] P. Ehrhard, S.H. Davis, Non-isothermal spreading of liquid drops on horizontal plates, J. Fluid Mech. 229 (1991) 365–388.
[23] E. Saiz, A.P. Tomsia, N. Rauch, C. Scheu, M. Ruehle, M. Benhassine, D. Seveno, J. De Coninck, S. Lopez-Esteban, Nonreactive spreading at high temperature: Molten metals and oxides on molybdenum, Phys. Rev. E 76 (2007) 041602.
[24] M.J. De Ruijter, J. De Coninck, G. Oshanin, Droplet spreading: Partial wetting regime revisited, Langmuir 15 (1999) 2209–2216.
[25] S. Su, L. Yin, Y. Sin, B.T. Murray, T.J. Singler, Modeling dissolution and spreading of Bi–Sn alloy drops on a Bi substrate, Acta Mater. 57 (2010) 3110–3122.
[26] O. Kozlova, R. Voytovych, N. Eustathopoulos, Initial stages of wetting of alumina by reactive CuAgTi alloys, Scr. Mater. 65 (2010) 13–16.